Journal of Geodynamics 122 (2018) 41–53

Contents lists available at ScienceDirect

Journal of Geodynamics

journal homepage: www.elsevier.com/locate/jog

Late Cretaceous to early Paleogene forearc magmatism and subduction initiation in the Paleo-Kuril arc-trench system, eastern Hokkaido, Japan

Yasuo Ikeda*, Motojiro Goto[1]

Kushiro Campus, Hokkaido University of Education, Kushiro, 085-8580, Hokkaido, Japan

ARTICLE INFO

Keywords:
Nemuro group
Paleo-Kuril arc
Forearc basin
Alkaline magma
Fluid
Phengite

ABSTRACT

New major and trace elemental data presented here imply a temporal and spatial change in the magmatic evolution and mode of subduction initiation in the Paleo-Kuril arc-trench system, eastern Hokkaido, Japan. Late Cretaceous to early Paleogene igneous rocks from the Nemuro Group (Nokkamappu, Hamanaka, and Kiritappu Formations) in the forearc basin of the Paleo-Kuril arc consist of the tholeiitic, alkaline and calc-alkaline rock series, based on petrographic and major-element (K_2O, total alkalies [$K_2O + Na_2O$], and SiO_2 contents) data. Immobile-element features on the Zr/TiO_2 vs. Nb/Y diagram indicate that a majority of the alkaline rocks are classified as non-alkaline rock. The low TiO_2 (< 1%), high V/Ti, and low Nb/Yb ratios of the igneous rocks show that the original mantle compositions of alkaline and non-alkaline rocks were highly refractory in nature. The magmas were produced with a 10–20% partial melting of the depleted mantle, which is common in arc-related non-alkaline magma. The high Th/Yb, Ba/La, Rb/La, and Ba/Th ratios and low La/Sm ratios of the alkaline and tholeiitic rocks from the Nokkamappu and Hamanaka Formations strongly reflect the imprint of substantial fluid components from the subducting slab. The enriched K and Rb in the alkaline magma source are indicative of fluid derived from mica breakdown. Cs fractionation in the slab-derived fluids is indicated by variations in Y/Cs and Nb/Cs, and the fluids are controlled by fluid derived from the breakdown of mica such as phengite. Tholeiitic and calc-alkaline rocks from the Kiritappu Formation show less aqueous fluids. Late Cretaceous magmatism, with decompression melting and formation of the forearc basin, resulted from rollback during subducting initiation, which was associated with a rift system created by the upwelling of depleted mantle following the onset of the sinking of the slab into the mantle. Subsequently, the rollback of the subducting slab slowed down and stabilized, and consequently, normal tholeiitic and calc-alkaline magmas were produced in the early Paleogene.

1. Introduction

The Pre-Cenozoic geologic framework of Hokkaido is divided into five stratigraphic-tectonic major belts, which are, from west to east, the Oshima-Rebun Belt, Sorachi-Yezo Belt, Hidaka Belt, Tokoro Belt, and Nemuro Belt (Kiminami and Kontani, 1983) (Fig. 1A). The late Cretaceous to early Paleogene Nemuro Group in the Nemuro Belt is distributed from the eastern end of the Nemuro Peninsula to Kushiro City in southeastern Hokkaido (Fig. 1B). The Nemuro Group is interpreted to represent forearc-basin deposits of the Paleo-Kuril subduction system along the southern margin of the Paleo-Okhotsk Land based on their sedimentary facies, the total thickness of which exceeds 3,000 m (Kiminami, 1983; Kiminami and Kontani, 1983; Naruse, 2003). Alkaline and non-alkaline rocks in the form of sills, dikes, and lava deposits, including pillow lavas and pyroclastics are exposed in the Nemuro Group (Mitani et al., 1958; Fujiwara and Mitani, 1959; Hasegawa and Mitani, 1959; Okazaki and Nagahama, 1965; Kiminami, 1978, 1983). This magmatism occurred concurrently with sedimentation of the Nemuro Group, and is regarded as a frontal arc sequence caused by subduction of the Kula or Pacific Plate (Kiminami, 1978, 1983; Kiminami and Kontani, 1983; Kimura and Tamaki, 1985; Ueda and Miyashita, 2005). New plate tectonics model reveals subduction of the Izanagi plate (Seton et al., 2012). The petrology of the late Cretaceous alkaline rocks of the Nemuro Peninsula (whole-rock geochemistry [major elements] and mineral chemistry) was first described by Yagi (1969), and further geochemical investigations of the intrusion and associated sills (whole-rock geochemistry [major and trace elements]) were conducted by Ishikawa et al. (1971); Takahashi (1978), and Yutani and Hirano

* Corresponding author. Present address: 1-6-1-729 Fuchinobe Chuo-ku, Sagamihara-city, Kanagawa, 252-0206, Japan.
E-mail address: ikeda@zb.cyberhome.ne.jp (Y. Ikeda).
[1] Present address: Takatsuki city Abu-san junior high school, 1-2-1 Nasahara Takatsuki city, Osaka prefecture, 569-1041, Japan.

https://doi.org/10.1016/j.jog.2018.11.002
Received 18 April 2018; Received in revised form 18 October 2018; Accepted 14 November 2018
Available online 16 November 2018

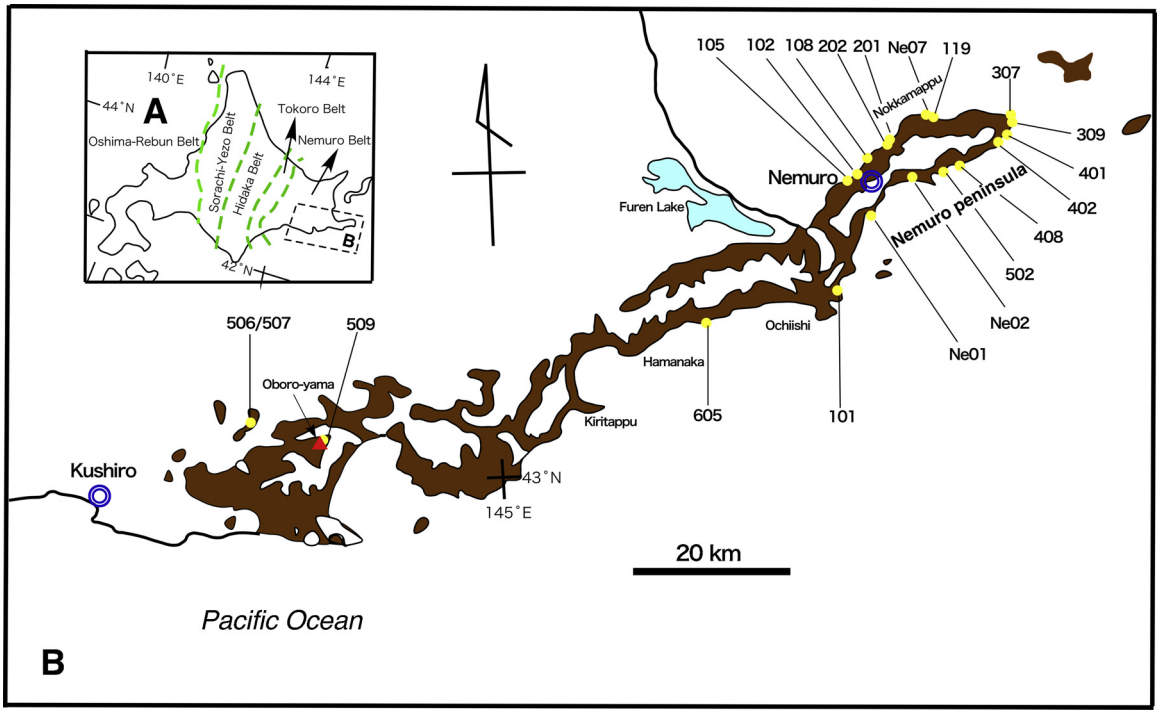

Fig. 1. Map showing the Pre-Cenozoic geologic framework of Hokkaido (modified after Kiminami and Kontani, 1983) (A) and distribution of the Nemuro Group (modified after Geological Survey of Hokkaido, 1980: painted in brown) and sampling locations (B).

Fig. 2. Outcrop photograph of the Hamanaka Formation at near the Ne01 point in Fig.1. Showing a transition from the lava sheet to pillow lavas at right end of the photograph.

(2015, 2016). Some alkaline rock sills occur as layered differentiated bodies (Yagi, 1969; Ishikawa et al., 1971). A more detailed magmatic fractionation (whole-rock geochemistry [major elements] and mineral chemistry) was presented by Simura and Ozawa (2006, 2011), focusing on compositional convection and crystal settling or flotation in the sills. The parent magma is inferred as potash-rich olivine basalt, likely derived from partial melting of phlogopite-peridotite in the upper mantle (Yagi, 1969; Ishikawa et al., 1971). However, it is still unclear why magmatism occurred beneath the forearc basin, and how the alkaline magma was produced. Furthermore, it is a mystery why there is no

Table 1
Major and trace element analyses of representative igneous rocks from the Nemuro Group.

Horizon	Nokkamappu Formation				Hamanaka Formation					
(Area)	(Nemuro)	(Nemuro)	(Kushiro)	(Kushiro)						
Sample No.	Ne07	119	506	507	105	102	108	202	201	307
Occurrence	pyroclastic rock	sill	lava	lava	sill	sill	sill	sill	sill	sill
Latitude (N)	43°23'30"	43°23'19"	43°4'51"	43°4'51"	43°19'29"	43°19'53"	43°21'1"	43°22'13"	43°22'16"	43°22'50"
Longitude (E)	145°39'20"	145°40'41"	144°37'12"	144°37'12"	145°33'9"	145°34'23"	145°35'31"	145°37'52"	145°37'54"	145°48'40"
Rock name	ol-px basalt	ol-px basalt	shoshonite	shoshonite	monzonite	shoshonite	shoshonite	shoshonite	ol-px basalt	shoshonite
Major elements (wt %)										
SiO_2	46.43	51.72	55.82	52.37	49.62	54.03	52.03	51.88	45.73	51.86
TiO_2	0.90	1.17	0.82	0.79	0.61	0.64	0.66	0.65	0.82	0.66
Al_2O_3	18.34	17.03	18.27	18.62	12.03	17.80	15.78	15.41	16.36	16.10
Fe_2O_3*	11.90	11.23	7.24	8.31	11.66	8.13	8.10	8.14	11.45	9.13
MnO	0.20	0.21	0.12	0.19	0.20	0.18	0.14	0.15	0.21	0.19
MgO	5.61	3.25	2.14	4.00	9.21	3.02	6.19	6.46	9.79	5.27
CaO	11.73	8.50	3.91	6.42	9.80	4.33	6.62	6.53	9.67	5.99
Na_2O	2.60	3.29	3.92	3.82	2.54	4.57	3.83	3.83	2.37	4.50
K_2O	0.58	1.35	5.47	3.21	2.76	4.69	3.98	4.11	0.83	3.50
P_2O_5	0.15	0.35	0.47	0.34	0.37	0.68	0.48	0.46	0.11	0.55
LOI	1.29	0.47	1.20	1.41	0.52	1.60	1.98	2.16	3.27	2.03
Total	99.73	98.56	99.38	99.48	99.31	99.66	99.80	99.76	100.62	99.78
Trace elements (ppm) by XRF										
V	384.8	309	175.4	308.2	246.1	167.6	227	223.3	375	253
Cr	30.2	10.7	3.1	4.4	364.7	16.6	252.4	256.9	211.4	113.6
Ni	19.2	7.1	2.9	3.5	116.5	12.3	108.2	119.7	61.6	49.6
Rb	11.3	22.3	81	46.4	58	75	67.7	66.6	5.6	56.7
Sr	552.3	484.2	864.5	1070.7	510.6	563.8	680.7	604.7	320.5	727.3
Ba	261.2	541.2	2084.4	1152.9	648.2	1060.8	845.8	1090.8	175.6	1268.9
Y	11.7	32.9	29.5	22.3	13.3	22.6	13.4	13.7	11.5	14.8
Zr	38.8	95	128.3	67.4	41	70.1	66.3	65.3	26.9	70.1
Nb	5.1	5.9	12.5	10.8	4	7	7	6.7	3.2	8.1
Trace elements (ppm) by ICP-MS										
Cs	0.2	0.2	0.3	0.4	1.5	2.2	1.2	1.8	< 0.1	3.8
La	5.97	10.7	24.4	14.5	5.99	14.4	15.9	14.2	3.2	18
Ce	13	25.5	48.4	29.9	13	29.3	29.9	26.4	7.78	34.1
Pr	1.8	3.85	6.23	3.97	1.83	3.94	3.55	3.13	1.18	4.09
Nd	8.92	18.3	26.4	17.5	8.35	16.6	14.1	12.1	6.05	16.3
Sm	2.39	4.99	6.22	4.32	2.34	4.2	3.23	2.75	1.86	3.62
Eu	0.861	1.48	1.72	1.38	0.799	1.31	1.05	0.917	0.705	1.12
Gd	2.49	5.52	5.73	3.98	2.47	4.23	2.79	2.61	2.15	3.12
Tb	0.41	0.95	0.91	0.62	0.38	0.66	0.44	0.42	0.36	0.46
Dy	2.47	5.76	5.25	3.61	2.3	3.88	2.57	2.39	2.17	2.59
Ho	0.5	1.17	1.06	0.71	0.47	0.78	0.53	0.47	0.44	0.51
Er	1.4	3.44	3.08	2.04	1.39	2.25	1.5	1.42	1.28	1.42
Tm	0.213	0.506	0.458	0.299	0.205	0.341	0.229	0.209	0.188	0.213
Yb	1.39	3.34	3.12	1.88	1.3	2.25	1.53	1.37	1.26	1.46
Lu	0.216	0.518	0.471	0.275	0.197	0.353	0.237	0.211	0.197	0.227
Hf	1	2.9	3.7	2.1	1.1	1.9	1.8	1.6	0.6	1.8
Ta	0.05	0.11	0.24	0.11	0.02	0.11	0.16	0.12	0.02	0.14
Pb	< 5	< 5	11	6	8	12	10	8	< 5	< 5
Th	0.68	1.21	3.65	2.15	1	1.99	2.81	2.4	0.36	3.08
U	0.25	0.61	1.13	0.69	0.47	0.75	1.1	0.98	0.15	1.22
Horizon	Hamanaka Formation								Kiritappu Formation	
(Area)									(Ochiishi)	(Oboro-yama)
Sample No.	309	401	402	408	502	Ne02	Ne01	605	101	509
Occurrence	sill	sill	sill	sill	sill	sill	pillow lava	sill	pyroclastic rock	dike
Latitude (N)	43°22'4"	43°21'45"	43°21'16"	43°19'44"	43°19'42"	43°19'15"	43°16'40"	43°10'29"	43°11'51"	43°2'13"
Longitude (E)	145°48'40"	145°48'5"	145°47'7"	145°43'40"	145°42'2"	145°36'55"	145°35'17"	145°19'54"	145°31'50"	144°40'25"
Rock name	monzonite	shoshonite	shoshonite	monzonite	shoshonite	shoshonite	shoshonite	shoshonite	andesite	hor andesite
Major elements (wt %)										
SiO_2	55.05	51.82	51.64	53.49	54.10	52.78	53.02	54.22	60.91	60.80
TiO_2	0.67	0.54	0.64	0.55	0.67	0.65	0.68	0.65	0.57	0.77
Al_2O_3	16.27	16.48	15.81	18.71	17.46	17.45	16.86	17.14	17.34	16.21
Fe_2O_3*	7.72	8.54	8.82	6.55	8.79	9.10	9.13	8.79	4.91	6.13
MnO	0.15	0.16	0.20	0.11	0.21	0.21	0.21	0.18	0.39	0.09
MgO	3.28	5.80	4.85	2.93	2.83	3.44	3.01	2.92	1.01	2.70
CaO	4.82	7.60	6.72	6.69	4.10	5.20	5.98	4.34	6.51	4.83
Na_2O	3.83	3.32	4.36	4.12	4.80	3.86	4.25	4.55	4.28	4.41
K_2O	5.81	3.55	3.36	4.28	4.45	4.55	4.18	4.26	2.07	2.46
P_2O_5	0.73	0.46	0.54	0.56	0.67	0.60	0.63	0.69	0.34	0.28
LOI	1.09	1.00	3.13	1.32	1.72	1.54	1.51	1.84	1.46	0.50
Total	99.41	99.27	100.08	99.31	99.81	99.38	99.44	99.58	99.78	99.17
Trace elements (ppm) by XRF										
V	212.9	198.2	237.4	184	187.4	196	206.4	177	49	163.5
Cr	72.5	247.9	106.2	70.8	6.1	7.1	9.9	23.8	3.8	33

(*continued on next page*)

Table 1 (*continued*)

Horizon	Nokkamappu Formation				Hamanaka Formation					
(Area)	(Nemuro)	(Nemuro)	(Kushiro)	(Kushiro)						
Ni	31.2	89.2	46.4	30.5	6.9	8.2	8.6	14.7	2.7	10.6
Rb	113.7	72.4	52.7	87.8	79.4	81.6	69.6	66	50.7	57
Sr	504.7	783.6	943.3	876.5	465.2	588.2	539.5	419.2	509.6	738.2
Ba	1210	912.4	1021.5	1039.8	1038.9	1123.4	1149.6	1328.2	557.9	708.6
Y	15.1	12.3	15.5	12.7	21.9	18.9	21.7	19.2	28	11.3
Zr	65.8	44.4	67.5	51.4	72.5	64.4	56	70.6	168.5	83.6
Nb	5.6	8.3	10.8	8.6	6	6.7	4.5	4.8	7.1	9
Trace elements (ppm) by ICP-MS										
Cs	1.9	1.9	1.2	2.5	1.9	1.3	0.4	1.1	1.9	1.1
La	9.97	6.85	17.7	7.92	12.7	12.4	12.6	13.3	15.4	16.7
Ce	20	14	32.9	15.9	26.4	26	26	27.1	36.3	36
Pr	2.63	1.84	3.95	2.13	3.54	3.49	3.48	3.62	4.75	4.36
Nd	11.4	8.04	15.8	8.98	15.5	15.1	15.8	15.7	19.9	17.5
Sm	2.7	2.13	3.23	2.39	3.75	3.73	3.87	3.85	4.8	3.59
Eu	0.894	0.729	1.1	0.772	1.21	1.21	1.22	1.17	1.32	1.04
Gd	2.7	2.1	2.94	2.15	3.6	3.65	3.67	3.67	4.41	2.66
Tb	0.44	0.33	0.45	0.35	0.58	0.61	0.62	0.61	0.79	0.4
Dy	2.58	2.08	2.55	2.13	3.39	3.57	3.52	3.59	4.77	2.1
Ho	0.52	0.41	0.49	0.41	0.7	0.71	0.71	0.72	0.94	0.39
Er	1.55	1.2	1.37	1.22	2.03	2.05	2.03	2.01	2.86	1.1
Tm	0.241	0.185	0.205	0.189	0.317	0.319	0.296	0.298	0.441	0.152
Yb	1.63	1.24	1.4	1.27	2.12	2.07	1.98	1.96	3.08	0.93
Lu	0.249	0.193	0.227	0.203	0.32	0.305	0.314	0.307	0.488	0.144
Hf	1.8	1.2	1.8	1.3	1.9	1.9	1.9	2	4.6	2.2
Ta	0.11	0.05	0.16	0.04	0.08	0.08	0.08	0.1	0.26	0.26
Pb	18	10	6	11	6	9	9	12	11	9
Th	1.82	1.13	3	1.36	1.98	1.77	1.76	2.01	3.64	3.92
U	0.91	0.55	1.22	0.65	0.81	0.69	0.76	0.81	1.25	1.37

ol: olivine, px: pyroxene, hor: hornblende, LOI: Loss on ignition.

magmatism equivalent to the volcanic front. It is well known that magmatism in a forearc setting is characterized by boninitic and tholeiitic (arc tholeiite or mid-ocean basalt [MORB]-like) rocks which are derived from very depleted mantle sources (e.g., Ewart and Bryan, 1972; Meijer, 1980; Miyake, 1985; Bloomer, 1987: Lytwyn et al., 1997; Mizoguchi et al., 2009; Yatsuka et al., 2010; Reagan et al., 2010; Imaoka et al., 2011). To our knowledge, there have been few reports of alkaline igneous activity within forearc basins.

Here, we collected samples from the entire area and horizon of the Nemuro Group and report comprehensive whole-rock major and trace element data for the late Cretaceous early Paleogene alkaline and non-alkaline rocks in the Group. We further discuss the tectonic implications of the presence of alkaline rocks within the forearc basin. The results provide insight into the geodynamic setting of the Paleo-Kuril arc–trench system.

2. Geological background and samples

The Nemuro Group strikes ENE-WSW or NE-SW and dips 10–25° gently to the south from the eastern end of the Nemuro Peninsula to Kushiro City (Kiminami, 1978). The deposits of this group are lithologically divided into the Nokkamappu, Otamura, Monshizu, Oborogawa, Hamanaka (Senpohshi in the Kushiro area), Akkeshi (Senpohshi in the Kushiro area), Tokotan, Kiritappu, Shiomi, Konbumori and Furubanya Formations in ascending order (Kiminami, 1978, 1983; Okada et al., 1987). The age of the basal strata of the Nemuro Group (Nokkamappu Formation) is Campanian to Maastrichtian age (Kiminami, 1983; Okada et al., 1987), and its lower limit is not known. Extrusive rocks (including pillow lava and pyroclastic rock) and intrusive rocks (sills and dikes) lie in the late Cretaceous Nokkamappu and Hamanaka and the early Paleogene Kiritappu Formations (Kiminami, 1978, 1983). A representative example of pillow lavas intercalated between alternating beds of sandstone and siltstone is shown in Fig. 2. Their modes of occurrence indicate that the pillow lava flows are evidently contemporaneous with sedimentation of the Nemuro Group (Yagi, 1969). Igneous rocks from the Nemuro Group consist of basalt, alkaline rocks, and andesite (Mitani et al., 1958; Fujiwara and Mitani, 1959; Hasegawa and Mitani, 1959; Okazaki and Nagahama, 1965; Yagi, 1969; Ishikawa et al., 1971; Takahashi, 1978; Yutani and Hirano, 2015, 2016; Simura and Ozawa, 2006, 2011). The K–Ar ages of alkaline rocks from the horizons of the Hamanaka Formation are 84–88 Ma (Ueda and Aoki, 1968). The K-Ar ages are old as compared to the biostratigraphic age of the Formation (Lower Maastrichtian: Naruse et al., 2000). The andesite dikes in the Oboro-yama area penetrate into the Senpohshi Formation (Okazaki and Nagahama, 1965). The ages of the intrusion are inferred to be horizons of the Kiritappu Formation, based upon the geological description of Okazaki and Nagahama (1965). The Kiritappu Formation is Danian in age (Kiminami, 1983; Okada et al., 1987).

The analyzed samples were collected from the three formations; sampling locations are shown in Fig. 1 and Table 1. Rock names in Table 1 are based on igneous rock textures (porphyritic or holocrystalline rock). The porphyritic rocks are further classified into various rock types based upon the classification of LeMaitre et al. (2002)

2.1. Nokkamappu formation

Nokkamappu Formation (Nemuro): The analyzed samples (pyroclastic rock and sill) from the Nokkamappu Formation in the Nemuro area are porphyritic olivine-pyroxene basalts (Fig. 3A). The most common phenocrysts are of plagioclase followed by clinopyroxene and olivine, in order of abundance. The matrix is intergranular in texture and consists of plagioclase, clinopyroxene, olivine, and opaque oxide minerals. Olivine in both the phenocrysts and matrix are replaced by chlorite. The petrographic features are indicative of the tholeiitic rock series.

Nokkamappu Formation (Kushiro): The analyzed samples (lava) from the Nokkamappu Formation in the Kushiro area are porphyritic shoshonites (Fig. 3B). The principal phenocrysts are of plagioclase and the next in abundance is clinopyroxene. The matrix is intergranular or pilotaxitic in texture and consists of plagioclase, clinopyroxene,

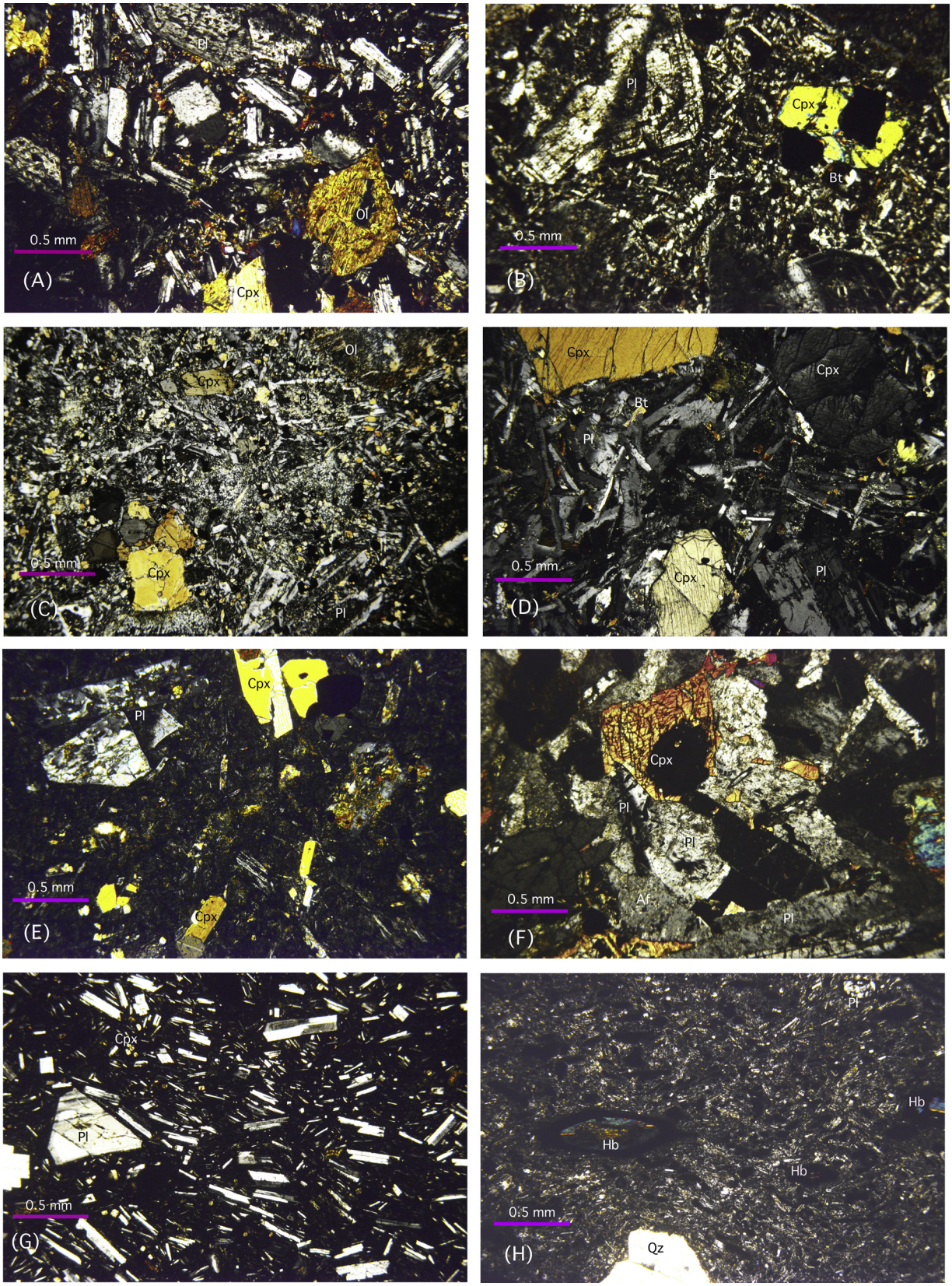

Fig. 3. Representative photomicrographs of the igneous rocks from the Nemuro Group (cross polarized light). (A) Basalt (Ne07: pyroclastic rock) from the Nokkamappu Formation (Nemuro area); (B) Shoshonite (507: lava) from the Nokkamappu Formation (Kushiro area); (C) Basalt (201: sill) from the Hamanaka Formation; (D) Shoshonite (108: sill) from the Hamanaka Formation; (E) Shoshonite (Ne01: pillow lava) from the Hamanaka Formation; (F) Monzonite (408: sill) from the Hamanaka Formation; (G) Andesite (101: pyroclastic rock) from the Kiritappu Formation (Ochiishi area); (H) Hornblende andesite (509: dike) from the Kiritappu Formation (Oboro-yama area). Ol, olivine; Cpx, clinopyroxene; Hb, hornblende; Bt, biotite; Pl, plagioclase; Af, alkali feldspar; Qz, quartz.

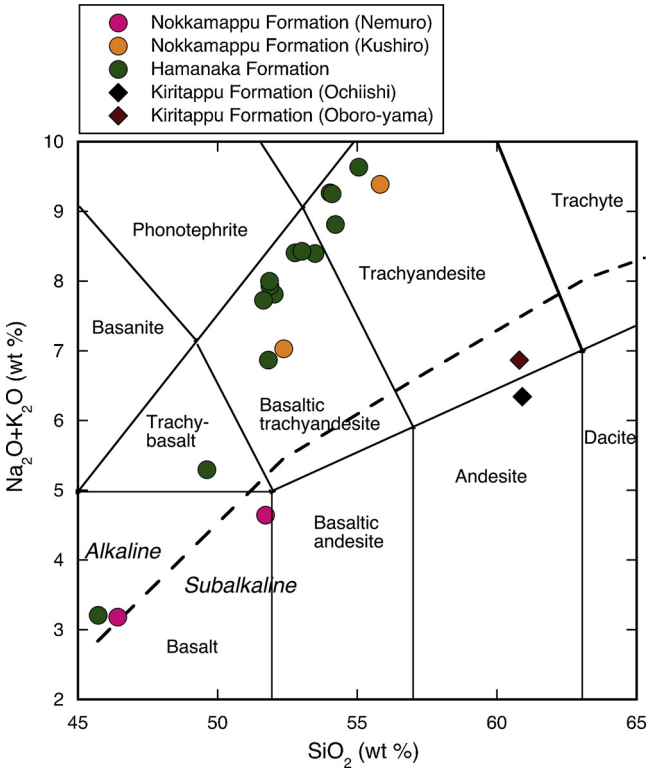

Fig. 4. Total alkali vs. SiO_2 classification diagram (LeMaitre et al., 2002) for samples from the Nemuro Group. The broken line shows the boundary between alkaline and subalkaline rocks after Irvine and Baragar (1971).

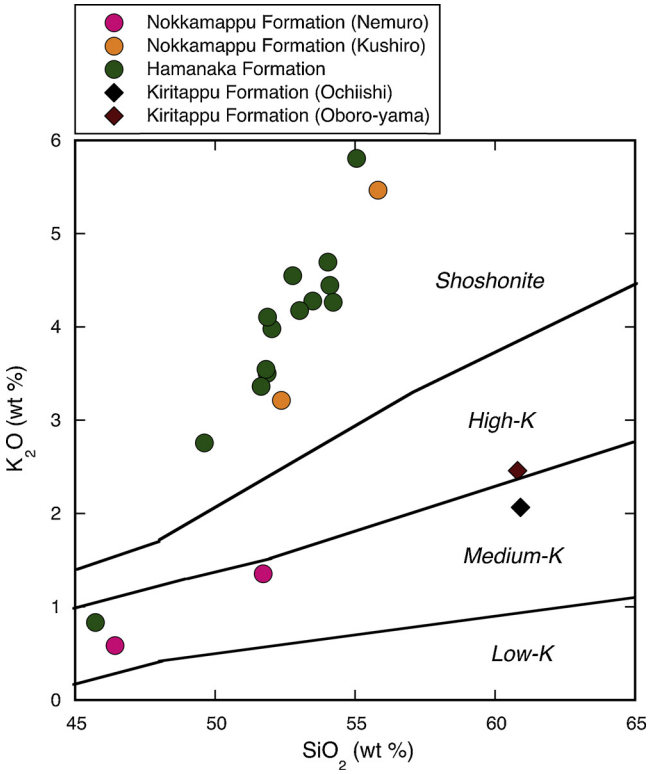

Fig. 5. K_2O vs. SiO_2 classification diagram (LeMaitre et al., 2002) for samples from the Nemuro Group.

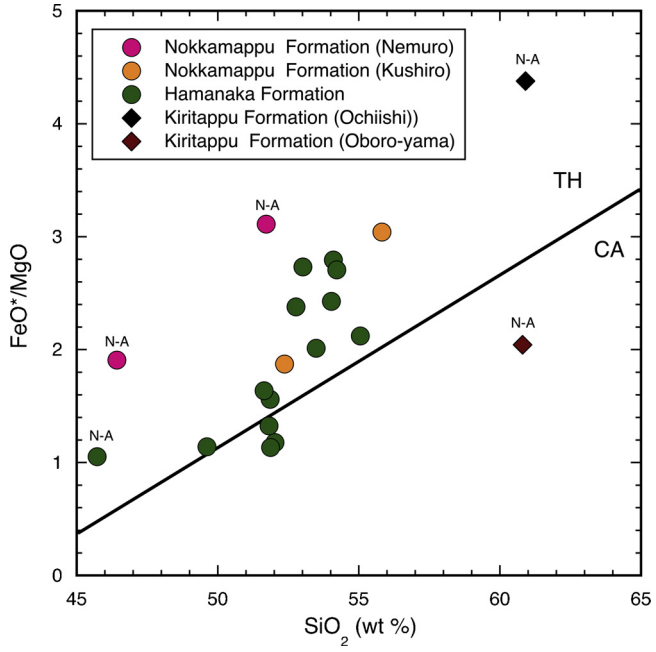

Fig. 6. FeO*/MgO vs. SiO_2 discriminant diagram (Miyashiro, 1974) for samples from the Nemuro Group. TH: tholeiitic, CA: calc-alkaline, N-A: non-alkaline rock.

chloritized biotite, and opaque oxide minerals.

2.2. Hamanaka formation

Igneous rocks occur as sills and lava deposits, including pillow lavas in the Formation, and consist of basalt, shoshonite, and monzonite.

Basalt (sill): The most common phenocrysts are of plagioclase followed by clinopyroxene and olivine, in order of abundance (Fig. 3C). The matrix is intergranular in texture and consists of plagioclase, clinopyroxene, olivine and opaque oxide minerals. The olivine in both the phenocrysts and matrix are replaced by chlorite. The petrographic features are indicative of the tholeiitic rock series.

Shoshonite (sill): The most common phenocrysts are of plagioclase followed in order of abundance by clinopyroxene, olivine (or absent) and biotite (or absent) (Fig. 3D). Olivine phenocrysts are replaced by chlorite. The matrix is intergranular in texture and consists of plagioclase, clinopyroxene, biotite (or absent), and opaque oxide minerals. Biotite in both the phenocrysts and matrix are frequently altered to chlorite.

Shoshonite (pillow lava): The phenocrysts are, in order of, abundance by plagioclase, clinopyroxene and olivine (Fig. 3E). The matrix is intersertal in texture and consists of plagioclase, clinopyroxene, and opaque oxide minerals. The olivine phenocrysts are replaced by chlorite.

Monzonite (sill): The holocrystalline rock is composed mainly of plagioclase and clinopyroxene with subordinate amounts of alkali feldspar, biotite and opaque oxide minerals (Fig. 3F).

2.3. Kiritappu formation

Kiritappu Formation (Ochiishi): The analyzed sample (pyroclastic rock) from the Kiritappu Formation in the Ochiishi area is porphyritic andesite (Fig. 3G). Plagioclase phenocrysts lie in a matrix of pilotaxitic texture with plagioclase, clinopyroxene, and opaque oxide minerals.

Kiritappu Formation (Oboro-yama): The analyzed sample (dike) from the Kiritappu Formation in the Oboro-yama area is porphyritic hornblende andesite (Fig. 3H). The phenocrysts are, in order of abundance, hornblende with a resorption border (or completely resorbed),

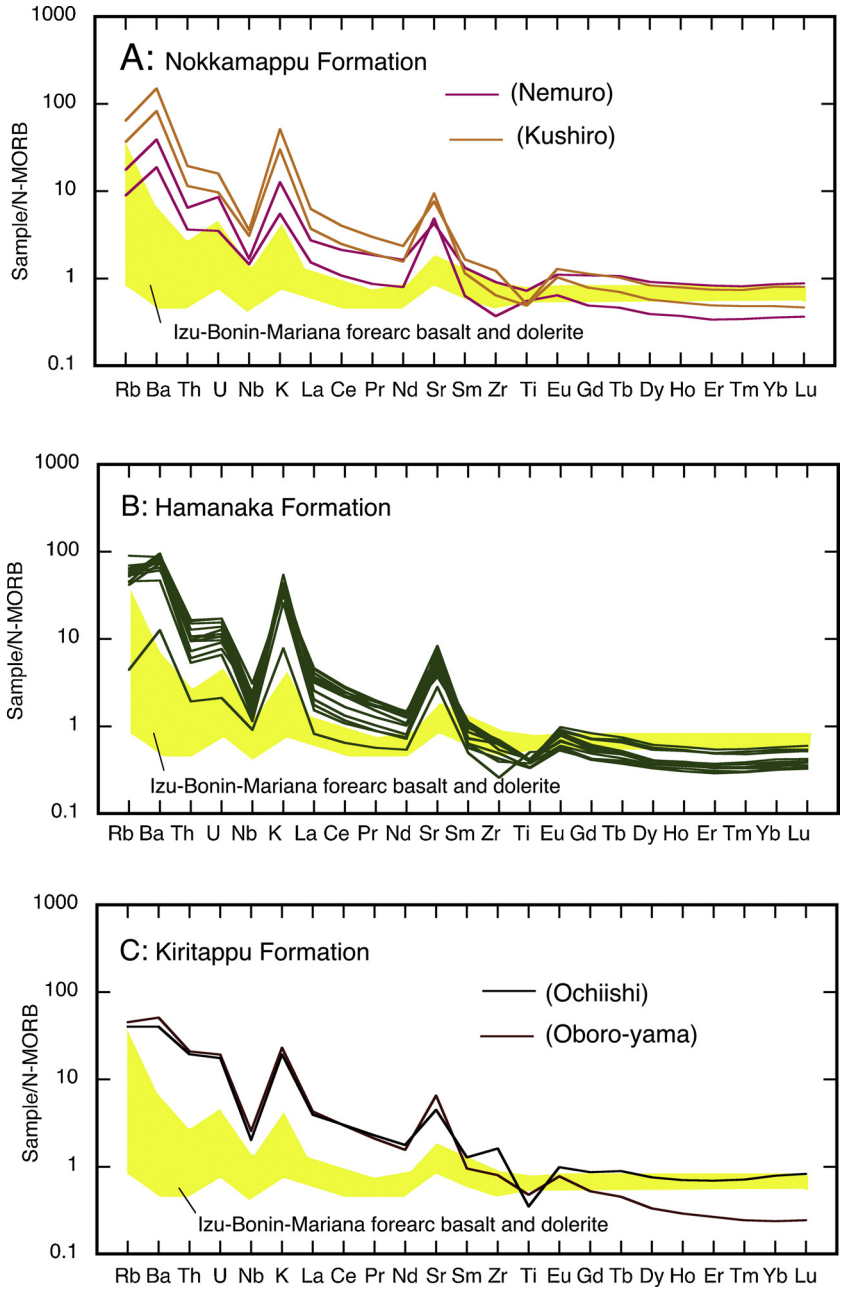

Fig. 7. N-MORB normalized incompatible element diagrams for samples from the Nemuro Group, arranged in order of elements becoming increasingly incompatible in the mantle to the left. Normalizing values from Hofmann (1988). The field for the Izu-Bonin-Mariana forearc basalt and dolerite is from Dai et al. (2013).

plagioclase, and partly corroded quartz. The matrix is pilotaxitic in texture and consists of plagioclase, completely resorbed hornblende, and opaque oxide minerals. The petrographic features indicate the calc-alkaline rock series.

3. Analytical procedures and results

Whole-rock major and trace element (V, Cr, Ni, Rb, Sr, Ba, Y, Zr, and Nb) concentrations were determined on fused glass beads using X-ray fluorescence spectrometry (*PANalytical MagiX*) at the Hokkaido University of Education, following the analytical procedures outlined by Miyamoto and Okamura (2003). Other trace element concentrations were measured at Activation Laboratories Ltd. (Ontario, Canada) by inductive coupled plasma–mass spectrometry (ICP–MS). The whole-rock data are shown in Table 1

3.1. Major element compositions

In the total alkali-silica classification diagram (LeMaitre et al., 2002), samples of the Nokkamappu Formation (Nemuro), and one sample each from the Hamanaka and Kiritappu (Ochiishi) Formations are plotted in the non-alkaline rock field (basalt and andesite), whereas other samples of the Nokkamappu (Kushiro), Hamanaka and Kiritappu (Oboro-yama) Formations have compositions of alkaline rocks (trachybasalt, basaltic trachyandesite and trachyandesite) (Fig. 4). A sample of the Kiritappu (Oboro-yama) Formation is classified as sub-alkaline rock, based on the classification of Irvine and Baragar (1971). On the K-silica classification diagram (LeMaitre et al., 2002), samples of the Nokkamappu (Nemuro) and Kiritappu (Ochiishi and Oboro-yama) Formations and one sample of the Hamanaka Formation are encompass medium-K to high-K basalt and andesite, and the other samples of the Nokkamappu (Kushiro) and Hamanaka Formations are plotted in the

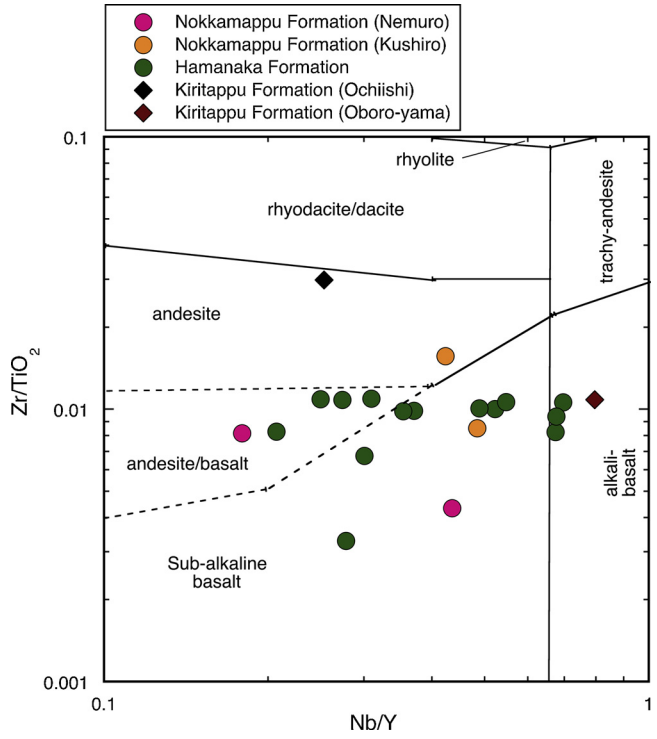

Fig. 8. Zr/TiO_2 vs. Nb/Y diagram (Winchester and Floyd, 1977) for samples of the Nemuro Group.

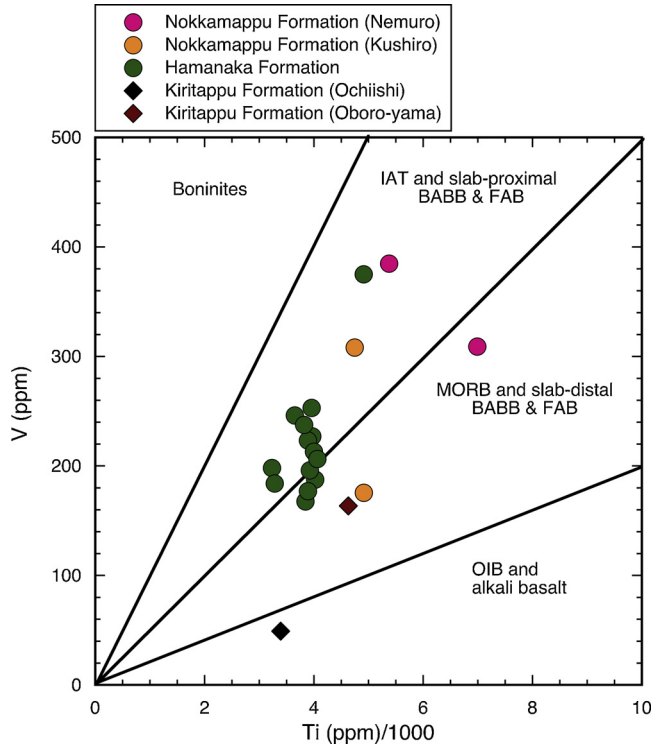

Fig. 9. V vs. Ti diagram (Shervais, 1982; Pearce, 2014) for samples from the Nemuro Group.

shoshonite field (Fig. 5). A sample from the Kiritappu (Oboro-yama) Formation falls into the calc-alkaline field on the FeO*/MgO vs. SiO_2 discriminant diagram (Miyashiro, 1974), as shown in Fig. 6, in contrast to the non-alkaline rocks from the Nokkamappu (Nemuro), Hamanaka, and Kiritappu (Ochiishi) Formations (subscript N-A in Fig. 6), and a majority of the alkaline rocks from the Nokkamappu (Kushiro) and

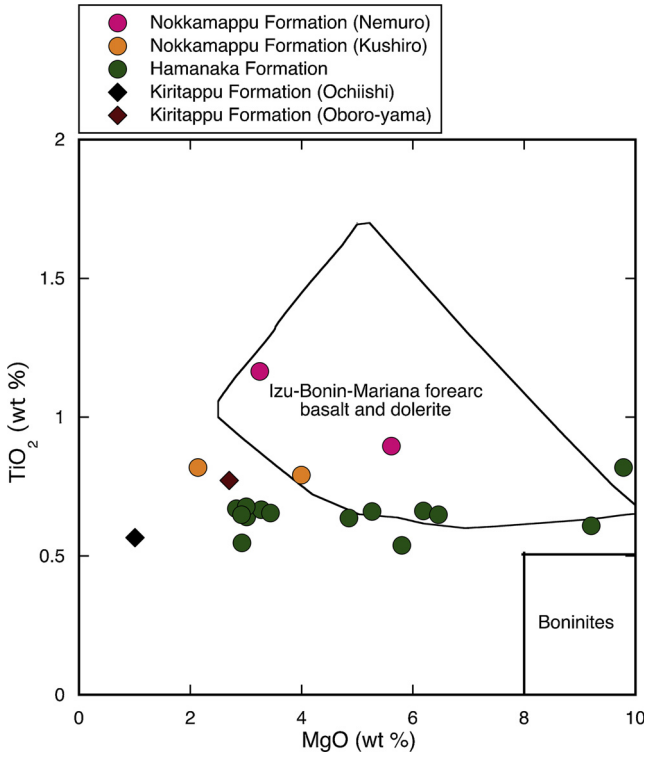

Fig. 10. TiO_2 vs. MgO diagram for samples from the Nemuro Group. The field for the Izu-Bonin-Mariana forearc basalt and dolerite is from Dai et al. (2013). The boninite field is based on contents of MgO and TiO_2 wt.% (Le Bas, 2000).

Hamanaka Formations, which are plotted in the tholeiitic field.

3.2. Trace element compositions

N-MORB-normalized (Hofmann, 1988) incompatible element variation diagrams for samples of the Nemuro Group (Fig. 7) show that they display enrichment in fluid-mobile large ion lithophiles (LILE; in particular, Rb, Ba, K, and Sr) and depletion in high field strength incompatible elements (HFSE: Ti, Nb, Zr, and heavy rare-earth elements) with negative Nb and Ti anomalies, as is typical of convergent margin magmatic suites. The trace element patterns confirm the enriched nature of the igneous rocks from the Nemuro Group, which have higher abundances of incompatible elements (Rb, Ba, Th, U, Nb, K, La, Ce, Pr, Nd, and Sr) than the Izu-Bonin-Mariana forearc basalt and dolerite (Fig. 7).

4. Discussion

The best model for the evolution of the Paleo-Kuril arc subduction system can explain the magmatism that occurred concurrently with the formation of the forearc basin. The discussion is concentrated on mantle source modeling, alkaline magma generation, and the geodynamic setting because these factors constrain for the tectono-magmatic evolution in the forearc area.

4.1. Original mantle compositions

The mantle source of the alkaline magma of the Nemuro Group has been inferred to have been enriched, such as the phlogopite–peridotite in the upper mantle (Yagi, 1969; Ishikawa et al., 1971). The composition of the underlying mantle of a subduction zone is known to be modified by the flux of hydrous fluids from the subducting slab. Elements of demonstrated immobility in hydrothermal alteration and metamorphism provide useful lithogeochemical parameters for the

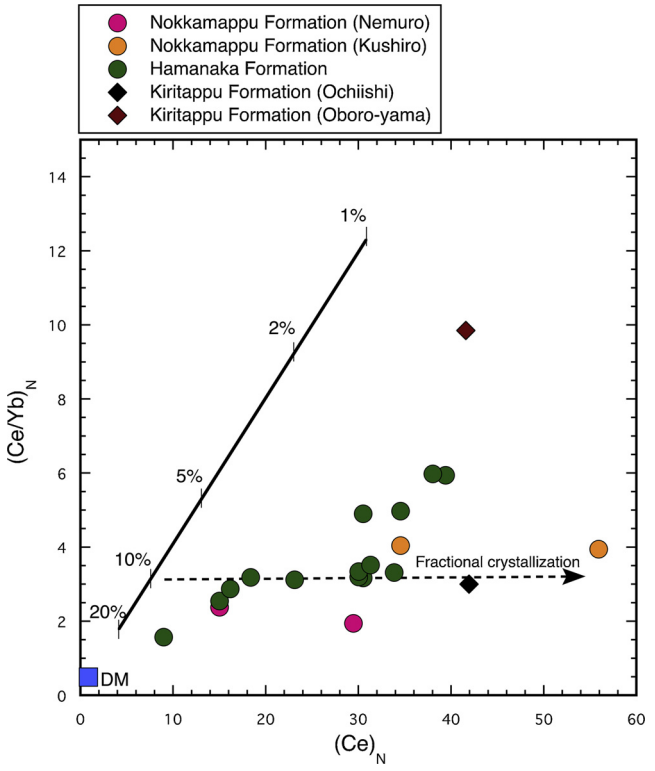

Fig. 11. Normalized $(Ce/Yb)_N$ vs. $(Ce)_N$ diagram during the partial melting a depleted mantle source (DM) for samples from the Nemuro Group. Partial melting curve between 1 and 20% is calculated using a batch melting model (Shaw, 1970). Chemical composition of depleted mantle (Ce = 0.772 ppm and Yb = 0.401 ppm), mineralogical composition of depleted mantle (55% olivine, 25% orthopyroxene, 11% clinopyroxene, and 9% garnet), mineral-melt distribution coefficients, and normalized values are taken from Rollinson (1993) and Salters and Stracke (2004).

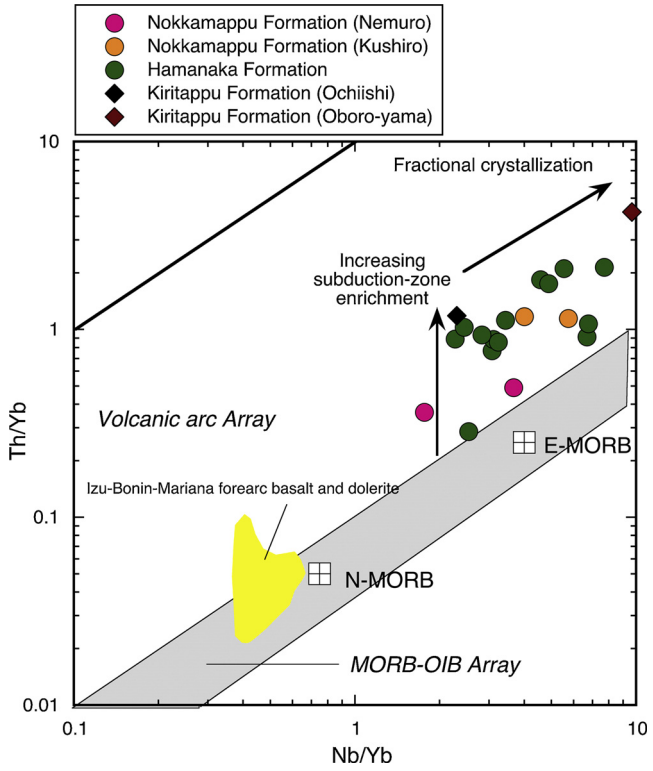

Fig. 12. Th/Yb vs. Nb/Yb diagram (Pearce, 2008) for samples from the Nemuro Group. The field for the Izu-Bonin-Mariana forearc basalt and dolerite is from Dai et al. (2013).

identifications of precursor volcanic rock types and magmatic affinities (e.g., MacLean and Barrett, 1993; Pearce, 2014).

Based on immobile trace element classification schemes, most samples from the Nemuro Group are non-alkaline rocks (sub-alkaline basalt, basalt, and andesite) according to the Zr/TiO_2 vs. Nb/Y diagram (Winchester and Floyd, 1977) (Fig. 8), which is incompatible with their major element compositions (Figs. 4 and 5). In the V vs. Ti diagram (Shervais, 1982; Pearce, 2014) (Fig. 9), a majority of the sample compositions from the Nemuro Group shift from intermediate V/Ti in MORB, forearc basalt (FAB) to island arc tholeiite (IAT) compositions, in contrast to a sample of tholeiitic rock from the Kiritappu Formation (Ochiishi), which is plotted with low V/Ti as containing an oceanic island basalt (OIB) composition. Samples from the Nemuro Group have low TiO_2 content (0.5–1.1 wt. %) and are plotted within the Izu–Bonin–Mariana forearc basalt and dolerite or near the boninitic field in the TiO_2 vs. MgO diagram (Le Bas, 2000; Dai et al., 2013) (Fig. 10). These geochemical features of immobile trace elements indicate that the original mantle compositions of alkaline and non-alkaline rocks from the Nemuro Group are highly refractory in nature. This conclusion is supported by the chemistry of detrital chromian spinels from the Eocene Urahoro Group in eastern Hokkaido, which unconformably overlies the Nemuro Group (Nanayama et al., 1994). These spinels are highly chromian Cr# (0.386–0.942), with high Mg# (0.253–0.751) and low TiO_2 content (0–0.38 wt.%), which imply that they originated in the forearc peridotites of the Paleo-Kuril arc-related depleted mantle.

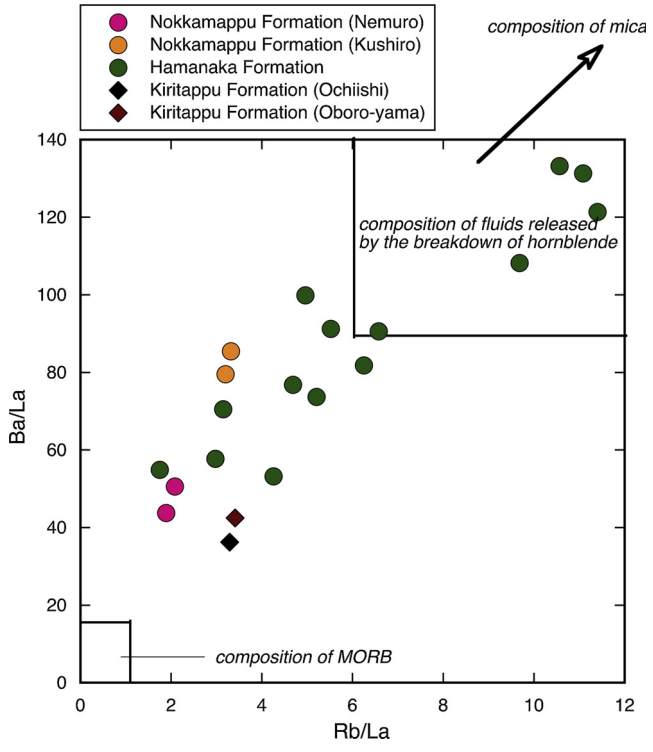

Fig. 13. Ba/La vs. Rb/La diagram with fields of composition of fluids released by the breakdown of hornblende and composition of MORB (Dupuy et al., 1982) for samples from the Nemuro Group. Compositions of mica are from Klemme et al. (2011).

4.2. Genesis of alkaline magma

How the alkaline magma is derived from the depleted mantle is the next essential problem. Magmas produced by low degrees of partial melting (less than approximately 10%) of the upper mantle are

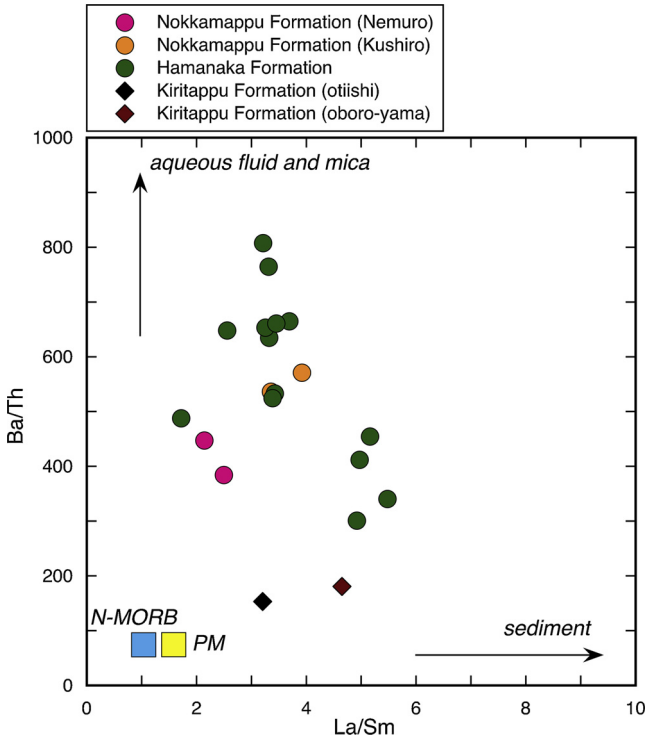

Fig. 14. Ba/Th vs. La/Sm diagram modified after Elliott (2003) for samples from the Nemuro Group. Compositions of N-MORB and primitive mantle (PM) are from Hofmann (1988), and mica compositions are from Klemme et al. (2011) and van Hinsberg et al. (2017).

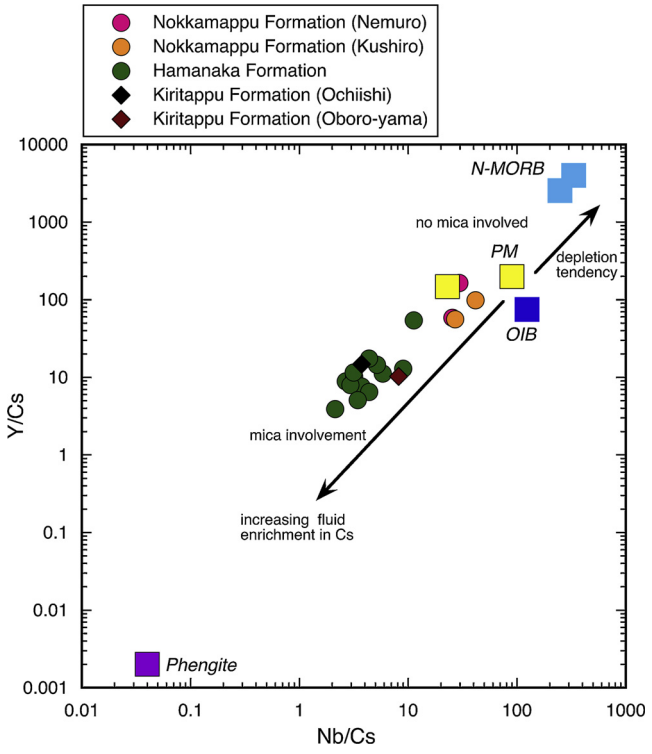

Fig. 15. Y/Cs vs. Nb/Cs diagram for samples from the Nemuro Group. Compositions of N-MORB, primitive mantle (PM) and oceanic island basalt (OIB) are from Hofmann (1988) and Sun and McDonough (1989), and phengite compositions are from van Hinsberg et al. (2017).

relatively enriched in incompatible elements such as K, Na, Rb, and Ba. For modeling the partial melting of the common mantle source, rare-earth element systematics are useful to process the identification of partial melting and fractional crystallization (Treuil and Varet, 1973; Allègre and Minster, 1978). The $(Ce/Yb)_N$ vs. $(Ce)_N$ diagram plots for samples from the Nemuro Group (Fig. 11) clearly enable such process identification. The partial melting curve is calculated using a batch melting model (Shaw, 1970). The chemical composition of the depleted mantle, mineralogical composition of depleted mantle, mineral-melt distribution coefficients, and normalized values are taken from Rollinson (1993) and Salters and Stracke (2004). In Fig. 11, with the exception of calc-alkaline rock from the Kiritappu Formation (Oboro-yama), samples from the Nokkamapu Formation (Nemuro and Kushiro), Hamanaka Formation, and the Kiritappu Formation (Ochiishi) reveal 10–20% partial melting of the depleted mantle and continue to show a fractional crystallization trend. This degree of partial melting is large compared with 1.5–11% partial melting for alkaline magma formation (e.g., Zou and Zindler, 1996; Caroff et al., 1997) and falls within 10–28% partial melting for arc-related non-alkaline magma formation (e.g. Gribble et al., 1998; Ulmer, 2001; Tamura et al., 2011). There is a slight possibility that the alkaline magma of the Nemuro Group could be produced in the low degree of partial melting model. Further insight into the genesis of calc-alkaline magma is left to future work.

As shown in Fig. 7, it is possible that the alkaline magmatism in the Nemuro Group was triggered by the addition of water-soluble elements such as K, Na, Rb, and Ba in the slab-derived aqueous fluids from the subducting slab. On the Th/Yb vs. Nb/Yb diagram (Pearce, 2008), samples from the Nemuro Group are plotted with low Nb/Yb ratios in the mantle array (MORB–OIB) and exhibit higher Th/Yb ratios than the array with subsequent fractional crystallization (Fig. 12). This finding indicates subduction components that were enriched in slab-derived fluids in the magmas and magma sources that were depleted, such as the MORB-type mantle (Pearce et al., 1995; Hawkesworth et al., 1997). The Nb/Yb ratios of the igneous rocks from the Nemuro Group are high as compared with those of the Izu-Bonin-Mariana forearc basalt and dolerite, which are E-MORB in character (Fig. 12). The Ba/La vs. Rb/La diagram (Fig. 13) shows the field of MORB as representative of a liquid produced from the normal upper mantle and the field of the calculated concentration of elements in hydrous fluids (Dupuy et al., 1982). The majority of samples from the Nemuro Group fall between the two fields and can be explained by interaction of these two components—fluids and either a MORB magma or depleted mantle source. Some samples from the Hamanaka Formation lie within the field of the composition of fluids released by the breakdown of hornblende. This process suggests fluids that are more enriched in Ba and Rb compositions such as mica. The Ba/Th vs. La/Sm diagram (Elliott, 2003) is useful in distinguishing two components responsible for much of the compositional variation observed in subduction zone magmas. High Ba/Th ratios indicate fluid involvement, given the contrasting fluid mobility of Ba and Th, whereas the La/Sm ratio is controlled by residual garnet in the slab; high values are ascribed to sediment melt (Elliott, 2003). Samples from the Nokkamappu and Hamanaka Formations have low La/Sm (2–6) and high Ba/Th (200–800) ratios in Fig. 14. It is suggested that the high Ba/Th ratios are characteristic of the strong addition of slab-derived fluids, including mica involvement (Klemme et al., 2011; van Hinsberg et al., 2017). In contrast, samples from the Kiritappu Formation have low Ba/Th ratios (< 200), which indicate less aqueous fluids.

Tamura et al. (2007); Kimura et al. (2010), and Ribeiro et al. (2013) have shown that the cause of elevated K and Rb in basaltic magma from the Izu-Bonin-Mariana Arc is the breakdown of phengite in the down-going slab. Melzer and Wunder (2000) and Green and Adam (2003) demonstrated that Cs strongly fractionates into coexisting fluids based on experimentally determined partition coefficients for LILE between fluids and phengite at high pressures (2–4 GPa) and low temperatures (600–700 °C). Tamura et al. (2007) have proposed a method of

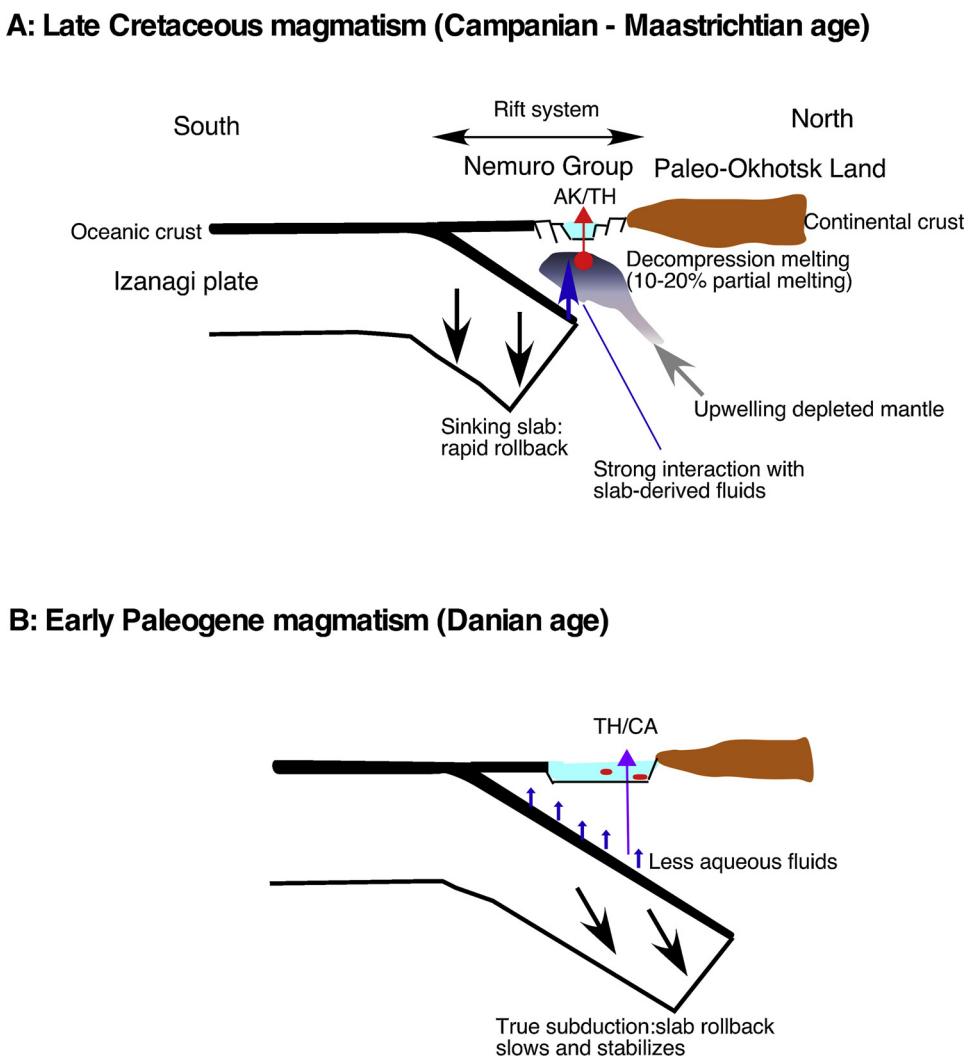

Fig. 16. Schematic model (not to scale) showing the processes of subduction initiation at the forearc of the Paleo-Kuril arc based on the models of Stern and Bloomer (1992); Bloomer et al. (1995); Stern (2004); Ishizuka et al. (2006, 2014b) and Dai et al. (2013). TH: tholeiitic magma, AK: alkaline magma, CA: calc-alkaline magma. See text for more details.

qualitatively estimating mica involvement based on the Ba/Cs vs. Rb/Cs diagram. To further discriminate aqueous fluids derived from mica, ratios of fluid-immobile elements (e.g., Nb and Y) to a fluid-mobile element (Cs) may provide good proxies for tracking the role of phengite breakdown in the slab. Thus, the Y/Cs vs. Nb/Cs diagram for samples from the Nemuro Group is shown in Fig. 15. The variation in Fig. 15 of N-MORB (Y/Cs = 2544–4000, Nb/Cs = 249–333: Hofmann, 1988; Sun and McDonough, 1989), primitive mantle (PM) (Y/Cs = 147–198, Nb/Cs = 23–90: Hofmann, 1988; Sun and McDonough, 1989), OIB (Y/Cs = 75, Nb/Cs = 124: Sun and McDonough, 1989), and phengite (Y/Cs = 0.002, Nb/Cs = 0.04: van Hinsberg et al., 2017) compositions exhibit positive correlation across a very wide range of values. Fluid addition to the mantle or magma source decreases Y/Cs and Nb/Cs, because Cs does not partition into phengite but strongly partitions into the fluid. Therefore, it is suggested that the variation between PM/OIB and phengite represents mica involvement, with no mica involved between PM/OIB and N-MORB. The variations in Y/Cs vs. Nb/Cs for samples from the Nemuro Group are very low compared with those of N-MORB, which indicates strongly increasing concentration in the slab fluids as phengite breaks down. The data cluster of alkaline rocks from the Hamanaka Formation shows the lowest Y/Cs and Nb/Cs values in the Nemuro Group, indicating the significant impact of fluid derived from phengite breakdown.

As previously indicated, variations in the degree of interaction with the original depleted mantle by hydrous fluids released from the descending slab are consistent with the main geochemical characteristics of alkaline and non-alkaline rocks from the Nemuro Group. The compositions of fluids are controlled by the breakdown of mica such as phengite, which results in the release of K, Rb, and Cs. Thus, high K content in alkaline rocks from the Hamanaka Formation are attributed to fluids derived from the mica breakdown into the magma source, whereas magma sources of tholeiitic and calc-alkaline rocks from the Nemuro Group are characterized by less aqueous fluid involvement.

4.3. Geodynamic setting and magmatic evolution

Recently, small-scale alkaline magmatism (OIB type) in a near-trench setting has been discovered in the outer zone of southwestern Japan and the northernmost Ryukyu Islands (Kiminami et al., 2017). The tectonic implications are similar to those of petit-spots, which are areas with small-scale magmatic activity (< 1 km in diameter) related to the occurrence of tensional fields in the lithosphere caused by plate flexure, with the ascending melt derived from a mantle source susceptible to partial melting (Hirano et al., 2006; Hirano, 2011). In contrast, large-scale alkaline magmatism (EW > 100 km, NS > 10 km) from the Nemuro Group (Fig. 1) represents arc-related magma

beneath the forearc basin. These observations cannot be accepted as the rendering of a tectonic model for petit-spots.

The geochemical features of the igneous rocks from the Nemuro Group in the forearc setting of the Paleo-Kuril arc, which indicate depleted sources (Figs. 7–10 and Fig. 12) and high concentrations of fluid-soluble elements (Figs. 12–14), are compatible with the model for the evolution of FAB from the Izu-Bonin-Mariana Arc (e.g., Reagan et al., 2010; Ishizuka et al., 2011, 2014). The presence of FAB and boninites is a major indicator of a subduction initiation forearc ridge (e.g., Reagan et al., 2010; Ishizuka et al., 2014a). Subduction initiation occurs in a forearc setting accompanied by initial sinking and ensuing slab rollback of a subducting plate (Stern and Bloomer, 1992; Bloomer et al., 1995; Stern, 2004; Dai et al., 2013). Slab rollback causes intense mantle diapirism and extension in the upper plate, during which decompression melting of the depleted mantle with fluids from the subducting slab generates the FAB and boninitic magmas (Stern and Bloomer, 1992; Bloomer et al., 1995; Stern, 2004; Dai et al., 2013; Ishizuka et al., 2006, 2014b). In this tectonic context, a schematic model (not to scale) for the tectonomagmatic evolution associated with the igneous rocks from the Nemuro Group at the forearc of the Paleo-Kuril arc is shown in Fig. 16. When the Izanagi plate (Seton et al., 2012) began to sink beneath the Okhotsk Plate (Paleo-Okhotsk Land) in the late Cretaceous (Kiminami, 1978, 1983; Kiminami and Kontani, 1983; Kimura and Tamaki, 1985; Ueda and Miyashita, 2005), formation of the tectonic basin of the rift system (commonly recognized as a forearc basin in this study area) occurred because of depleted mantle upwelling and decompression melting of the hydrous mantle (10–20% partial melting) in the extensional setting above the upper plate through the rapid rollback of the subducting slab (Fig. 16A: Campanian to Maastrichtian age). Reviewing the age of the basal strata of the Nemuro Group, it can be presumed that the formation of the tectonic basin began in the Pre-Campanian. The partial melting generated the alkaline and tholeiitic magmas. Variable degrees of hydration derived from the breakdown of mica, such as phengite from the sinking slab are required to explain the compositional variability of the magma types (from tholeiitic to alkaline magma) (Fig. 16A). With continued subduction, the subducting slab became stabilized because of slow rollback, and slab-derived fluids triggered the generation of normal tholeiitic and calc-alkaline magmas in the early Paleogene (Fig. 16B: Danian age).

5. Conclusions

The conclusions reached in this study can be summarized as follows:

1) Late Cretaceous to early Paleogene igneous rocks from the Nemuro Group in the forearc basin of the Paleo-Kuril arc consist of tholeiitic, alkaline, and calc-alkaline rock series, based on petrographic and major-element (K_2O, total alkalies [$K_2O + Na_2O$], and SiO_2 content) data.
2) Immobile-element features on the Zr/TiO_2 vs. Nb/Y diagram indicate that a majority of the alkaline rocks can be classified as non-alkaline rock.
3) The low TiO_2 (< 1%), high V/Ti, and low Nb/Yb ratios of the igneous rocks show that the original mantle compositions of the alkaline and non-alkaline rocks were highly refractory in nature. The magmas were produced with 10–20% partial melting of the depleted mantle, which is common in arc-related non-alkaline magma.
4) High Th/Yb, Ba/La, Rb/La, and Ba/Th ratios and low La/Sm ratios of the igneous rocks from the Nokkamappu and Hamanaka Formations strongly indicate the imprint of substantial fluid components from the subducting slab. K and Rb enrichment in the alkaline magma source is indicative of the fluid-induced breakdown of mica. Cs fractionation in the slab-derived fluids showed Y/Cs and Nb/Cs ratio variations, and the fluids were derived from breakdown of mica such as phengite. Tholeiitic and calc-alkaline rocks from the Kiritappu Formation exhibit less aqueous fluids.
5) Late Cretaceous magmatism associated with decompression melting and formation of the forearc basin resulted from rollback during subducting initiation, which was associated with the rift system caused by upwelling of depleted mantle following the onset of sinking of the slab into the mantle. Subsequently, the rollback of the subducting slab slowed and stabilized; consequently, normal tholeiitic and calc-alkaline magmas were produced in the early Paleogene.

Acknowledgments

We are grateful to S. Okamura for providing XRF measurements. Thanks are due to K. Kiminami, who provided suggestions during the preparation of this article. A part of this study includes the result of the graduation thesis by M. Goto, who is a coauthor of this paper. We thank an anonymous reviewer and Editor Irina Artemieva for their valuable comments and constructive suggestions, which significantly improved the manuscript. This research did not receive any specific grant from funding agencies in the public, commercial, or not-for-profit sectors. Finally, this article is respectfully dedicated to the late Dr. Kenzo Yagi.

References

Allègre, C.J., Minster, J.F., 1978. Quantitative models of trace element behavior in magmatic processes. Earth Planet. Sci. Lett. 38, 1–25.
Bloomer, S.H., 1987. Geochemical characteristics of boninite- and tholeiite- series volcanic rocks from the Mariana forearc and the role of an incompatible element-enriched fluid in arc petrogenesis. Geol. Soc. Am. Spec. Pap. 215, 151–164.
Bloomer, S.H., Taylor, B., MacLeod, C.J., Stern, R.J., Fryer, P., Hawkins, J.W., Johnson, L., 1995. Early arc volcanism and the ophiolite problem: a perspective from drilling in the western pacific. In: Taylor, B., Natland, J. (Eds.), Active Margins and Marginal Basins of the Western Pacific. Geophysical Monograph 88, Washington DC, pp. 1–30.
Caroff, M., Maury, R.C., Guille, G., Cotton, J., 1997. Partial melting below Tubuai (Austral Islands, French Polynesia). Contrib. Miner. Petrol. 127, 369–382.
Dai, J., Wang, C., Polat, A., Santosh, M., Li, Y., Ge, Y., 2013. Rapid forearc spreading between 130 and 120 Ma: evidence from geochronology and geochemistry of the Xigaze ophiolite, southern Tibet. Lithos 172-173, 1–16. https://doi.org/10.1016/j.lithos.2013.03.011.
Dupuy, C., Dostal, J., Marcelot, G., Bougault, H., Joron, J.L., Treuil, M., 1982. Geochemistry of basalts from central and southern New Hebrides arc: implication for their source rock composition. Earth Planet. Sci. Lett. 60, 207–225.
Elliott, T., 2003. Tracers of the slab. In: Eiler, J. (Ed.), Inside the Subduction Factory. American Geophysical Union, Geophysical Monograph 138, Washington DC, pp. 23–45.
Ewart, A., Bryan, W.B., 1972. Petrography and geochemistry of the igneous rocks from Eua, Tongan Islands. Geol. Soc. Am. Bull. 83, 3281–3298.
Fujiwara, T., Mitani, K., 1959. Explanatory Text of the Geological Map of Japan "Nosappu" (Scale, 1:50,000). Geol. Surv, Hokkaido, pp. 42 (in Japanese with English abstract 4p).
Geological Survey of Hokkaido, 1980. Geology and Resources of Hokkaido I Geology of Hokkaido "Geological Map of Hokkaido" (Scale 1: 600,000). Geol. Surv, Hokkaido, pp. 113 (in Japanese).
Green, T.H., Adam, J., 2003. Experimentally-determined trace element characteristics of aqueous fluid from partially dehydrated mafic oceanic crust at 3.0 GPa, 650-700°C. Eur J. Mineral. 15, 815–830. https://doi.org/10.1127/0935-1221/2003/0015-0815.
Gribble, R.F., Stern, R.J., Newman, S., Bloomer, S.H., O'Hearn, T., 1998. Chemical and isotopic composition of lavas from the northern Mariana trough: implications for magmagenesis in back-arc basins. J. Petrol. 39, 125–154.
Hasegawa, K., Mitani, K., 1959. Explanatory Text of the Geological Map of Japan "Nemurohokubu" (Scale, 1:50,000). Geol. Surv, Hokkaido, pp. 24 (in Japanese with English abstract 3p).
Hawkesworth, C.J., Turner, S.P., McDermott, F., Peate, D.W., van Calsteren, P., 1997. U-Th isotopes in arc magmas: implications for element transfer from the subducted crust. Science 276, 551–555.
Hirano, N., 2011. Petit-spot volcanism: a new type of volcanic zone discovered near a trench. Geochem. J. 45, 157–167.
Hirano, N., Takahashi, E., Yamamoto, J., Abe, N., Ingle, S.P., Kaneoka, I., Hirata, T., Kimura, J.-I., Ishii, T., Ogawa, Y., Machida, S., Suyehiro, K., 2006. Volcanism in response to plate flexure. Science 313, 1426–1428.
Hofmann, A.W., 1988. Chemical differentiation of the Earth: the relationship between mantle, continental crust, and oceanic crust. Earth Planet. Sci. Lett. 90, 297–314.
Imaoka, T., Kiminami, K., Nishida, K., Takemoto, M., Ikawa, T., Itaya, T., Kagami, H., Iizumi, S., 2011. K-Ar age and geochemistry of the SW Japan Paleogene cauldron cluster: implications for Eocene-Oligocene thermo-tectonic reactivation. J. Asian Earth Sci. 40, 509–533. https://doi.org/10.1016/j.jseaes.2010.10.002.
Ishizuka, O., Kimura, J.-I., Li, Y.B., Stern, R.J., Reagan, M.K., Taylor, R.N., Ohara, Y., Bloomer, S.H., Ishii, T., Hargrove III, U.S., Haraguchi, S., 2006. Early stages in the evolution of Izu-Bonin arc volcanism: new age, chemical and isotopic constraints. Earth Planet. Sci. Lett. 250, 385–401.

Ishizuka, O., Tani, K., Reagan, M.K., Kanayama, K., Umino, S., Harigane, Y., Sakamoto, I., Miyajima, Y., Yuasa, M., Dunlkley, D.J., 2011. The timescales of subduction initiation and subsequent evolution of an oceanic island arc. Earth Planet. Sci. Lett. 306, 229–240.
Ishizuka, O., Tani, K., Reagan, M.K., 2014a. Izu-Bonin-Mariana forearc crust as a modern ophiolite analogue. Elements 10, 115–120.
Ishizuka, O., Umino, S., Taylor, R.N., Kanayama, K., 2014b. Evidence for hydrothermal activity in the earliest stages of intraoceanic arc formation: implication to ophiolite-hosted hydrothermal activity. Econ. Geol. 109, 2159–2177.
Irvine, T.N., Baragar, W.R.A., 1971. A guide to the chemical classification of the common volcanic rocks. Can. J. Earth Sci. 8, 523–548.
Ishikawa, H., Berman, S., Yagi, K., 1971. Geochemical study of trace alements in the alkali rocks of Nemuro peninsula, Hokkaido. Japan. Geochem. J. 5, 187–206.
Kiminami, K., 1978. Stratigraphic re-examination of the Nemuro Group. Earth Science (Chikyu Kagaku) 32, 120–132 (in Japanese with English abstract).
Kiminami, K., 1983. Sedimentary history of the late Cretaceous – Paleocene Nemuro Group, Hokkaido, Japan: a forearc basin of the Paleo-Kuril arc-trench system. J. Geol. Soc. Japan 89, 607–624.
Kiminami, K., Imaoka, T., Ogura, K., Kawabata, H., Ishizuka, H., Mori, Y., 2017. Tectonic implications of Early Miocene OIB magmatism in a near-trench setting: the outer zone of SW Japan and the northernmost Ryukyu. J. Asian Earth Sci. 135, 291–302. https://doi.org/10.1016/j.jseaes.2016.12.033.
Kiminami, K., Kontani, Y., 1983. Mesozoic arc-trench systems in Hokkaido, Japan. In: Hashimoto, M., Uyeda, S. (Eds.), Accretion Tectonics in the Circum-Pacific Regions. Terrapub, Tokyo, pp. 107–122.
Kimura, G., Tamaki, K., 1985. Tectonic framework of the Kuril arc since its initiation. In: Nasu, N., Uyeda, S., Kobayashi, K., Kushiro, I., Kagami, H. (Eds.), Formation of Active Ocean Margins. Terrapub, Tokyo, pp. 641–676.
Kimura, J.-I., Kent, A.J., Rowe, M.C., Katakuse, M., Nakano, F., Hacker, B.R., van Keken, P.E., Kawabata, H., Stern, R.J., 2010. Origin of cross-chain geochemiocal variation in Quaternary lavas from the northern Izu arc: using a quantitative mass balance approach to identify mantle sources and mantle wedge processes. Geochem. Geophys. Geosyst. 11, Q10011. https://doi.org/10.1029/2010GC003050.
Klemme, S., Marschall, H.R., Jacob, D.E., Prowatke, S., Ludwig, T., 2011. Trace-element partitioning and Boron isotope fractionation between white mica and tourmaline. Canadian Mineralo. 49, 165–176.
Le Bas, M.J., 2000. IUGS reclassification of the high-Mg and picritic volcanic rocks. J. Petrol. 41, 1467–1470.
LeMaitre, R.W. (Ed.), Streckeisen, A., Zanettin, B., Lebas, M.J., Bonin, B., Bateman, P., Bellieni, G., Dudek, A., Efremova, S., Keller, J., Lameyre, J., Sabine, P.A., Schmid, R., Sørensen, H., Woolley, A.R., 2002. Igneous rocks: A classification and glossary of terms. Cambridge University Press, Cambridge, New York, Melbourne, 236p.
Lytwyn, J., Casey, J., Gilbert, S., Kusky, T., 1997. Arc-like mid-ocean ridge basdalt formed seaward of a trench-forearc system just prior to ridge subduction: An example from subaccreted ophiolites in southern Alaska. J. Geophy. Res. 102, 10225–10243.
MacLean, W.H., Barrett, T.J., 1993. Lithogeochemical techniques using immobile elements. J. Geochem. Explor. 48, 109–133.
Meijer, A., 1980. Primitive island arc volcanism and a boninite series: examples from western pacific islan arcs. In: Hayes, D.E. (Ed.), The Tectonic and Geologic Evolution of Southeast Asian Seas and Islands. Geophys. Monogr. Ser. 23, Washington, D.C, pp. 271–282.
Melzer, S., Wunder, B., 2000. Island-arc basalt alkali ratios: constraints from phengite-fluid partitioning experiments. Geology 28, 583–586.
Mitani, K., Fujiwara, T., Hasegawa, K., 1958. Explanatory Text of the Geological Map of Japan “Nemuronanbu” (Scale, 1:50,000). Geol. Surv, Hokkaido, pp. 35 (in Japanese with English abstract 5p).
Miyake, Y., 1985. MORB-like tholeiites formed within the Miocene forearc basin, southwest Japan. Lithos 18, 23–34.
Miyamoto, Y., Okamura, S., 2003. High-accuracy analysis of major and trace elements for geological samples using X-ray fluorescence spectrometry. J. Hokkaido Univ. Edu. Nat. Sci. 54, 49–59.
Miyashiro, A., 1974. Volcanic rock series in island arcs and active continental margins. Am. J. Sci. 274, 321–355.
Mizoguchi, S., Kiminami, K., Imaoka, T., Kamei, A., 2009. Miocene near-trench magmatism in the Cape Muroto area, shikoku, SW Japan. J. Geol. Soc. Japan 115, 17–30 (in Japanese with English abstract).
Nanayama, F., Nakagawa, M., Okada, H., 1994. Chemistry of detrital chromian spinels from the Eocene Urahoro Grouo, in the eastern Hokkaido and its origin. J. Geol. Soc. Japan 100, 383–398 (in Japanese with English abstract).
Naruse, H., Maeda, H., Shigeta, Y., 2000. Newly discovered Late Cretaceous molluscan fossils and inferred K/T boundary in the Nemuro Group, eastern Hokkaido, northern Japan. J. Geol. Soc. Japan 106, 161–164 (in Japanese with English abstract).
Naruse, H., 2003. Cretaceous to Paleocene depositional history of North-Pacific subduction zone: reconstruction from the Nemuro Group, eastern Hokkaido, northern Japan. Cretaceous Res. 24, 55–71. https://doi.org/10.1016/S0195-6671(03)00024-7.
Okada, H., Yamada, M., Matsuoka, H., Murota, T., Isobe, T., 1987. Calcareous nannofossils and biostratigraphy of the upper Cretaceous and lower Paleogene Nemuro Group, eastern Hokkaido, Japan. J. Geol. Soc. Japan 93, 329–348.
Okazaki, Y., Nagahama, H., 1965. Explanatory Text of the Geological Map of Japan “Oboro” (Scale, 1:50,000). Geol. Surv, Hokkaido, pp. 65 (in Japanese with English abstract 6p).
Pearce, J.A., 2008. Geochemical fingerprinting of oceanic basalts with applications to ophiolite classification and the search for Archean oceanic crust. Lithos 100, 14–48.
Pearce, J.A., 2014. Immobile element fingerprinting of ophiolites. Elements 10, 101–108.
Pearce, J.A., Baker, P.E., Harvey, P.K., Luff, I.W., 1995. Geochemical evidence for subduction fluxes, mantle melting and fractional crystallization beneath the South Sandwich island arc. J. Petrol. 36, 1073–1109.
Reagan, M.K., Ishizuka, O., Stern, R.J., Kelley, K.A., Ohara, Y., Blichert-Toft, J., Bloomer, S.H., Cash, J., Fryer, P., Hanan, B.B., Hickey-Vargas, R., Ishii, T., Kimura, J., Peate, D.W., Rowe, M.C., Woods, M., 2010. Fore-arc basalts and subduction initiation in the Izu-Bonin-Mariana system. Geochem. Geophys. Geosyst. 11https://doi.org/10.1029/2009GC002871. Q03X12.
Ribeiro, J.M., Stern, R.J., Kelley, K.A., Martinez, F., Ishizuka, O., Manton, W.I., Ohara, Y., 2013. Nature and distribution of slab-derived fluids and mantle sources beneath the Southeast Mariana forearc rift. Geochem. Geophys. Geosyst. 14, 4585–4607.
Rollinson, H.R., 1993. Using Geochemical Data: Evaluation, Presentation, Interpretation. Longman Scientific & Technical, Essex, England; John Wiley & Sons, New York, pp. 352.
Salters, V.J.M., Stracke, A., 2004. Composition of the depleted mantle. Geochem. Geophys. Geosyst. 5https://doi.org/10.1029/2003GC000597. Q05B07.
Seton, M., Müller, R.D., Zahirovic, S., Gaina, C., Torsvik, T., Shephard, G., Talsma, A., Gurnis, M., Turner, M., Maus, S., Chandler, M., 2012. Global continental and ocean basin reconstructions since 200 Ma. Earth-Sci. Rev. 113, 212–270.
Shaw, D.M., 1970. Trace element fractionation during anatexis. Geochim. Cosmochim. Acta 34, 237–243.
Shervais, J.W., 1982. Ti-V plots and the petrogenesis of modern and ophiolitic lavas. Earth Planet. Sci. Lett. 59, 101–118.
Simura, R., Ozawa, K., 2006. Mechanism of crystal redistribution in a sheet-like magma body: constraints from the Nosappumisaki and other shoshonite intrusions in the Nemuro peninsula, noethern Japan. J. Petrol. 47, 1809–1851.
Simura, R., Ozawa, K., 2011. Magmatic fractionation by compositional convection in a sheet-like magma body: constraints from the Nosappumisaki intrusion, noethern Japan. J. Petrol 52, 1887–1925.
Stern, R.J., 2004. Subdution initiation: spontaneous and induced. Earth Planet. Sci. Lett. 226, 275–292.
Stern, R.J., Bloomer, S.H., 1992. Subduction zone infancy: example from the eocene izu-bonin-Mariana and jurassic California arcs. Geol. Soc. Am. Bull. 104, 1621–1636.
Sun, S., McDonough, W.F., 1989. Chemical and isotopic systematics of oceanic basalts: implications for mantle composition and processes. In: Saunders, A.D., Norry, M.J. (Eds.), Magmatism in the Ocean Basins. Geol. Soc. Spec. Publ. 42, London, pp. 313–345.
Takahashi, S., 1978. Petrology of Alkali Dolerite in Nemuro Peninsula. MSc thesis. Hokkaido University (in Japanese), Sapporo.
Tamura, Y., Ishizuka, O., Stern, R.J., Shukuno, H., Kawabata, H., Embley, R.W., Hirahara, Y., Chang, Q., Kimura, J.-I., Tatsumi, Y., Nunokawa, A., Bloomer, S.H., 2011. Two primary basalt magma types from northwest Rota-1 volcano, Mariana arc and its mantle diaper or mantle wedge plume. J. Petrol. 52, 1143–1183.
Tamura, Y., Tani, K., Chang, Q., Shukuno, H., Kawabata, H., Ishizuka, O., Fiske, R.S., 2007. Wet and dry basalt magma evolution at Torishima volcano. Izu-Bonin arc, Japan: the possible role of phengite in the downgoing slab. J. Petrol. 48, 1999–2031.
Treuil, M., Varet, J., 1973. Criteres volcanologiques, petrologiques et geochimiquede la genese et de la differenciation des magmas basaltiques: exemple de l’Afar. Bul. Geol. Geol. France, 7th ser. 15, 506–540.
Ueda, H., Miyashita, S., 2005. Tectonic accretion of a subducted intraoceanic remnant arc in Cretaceous Hokkaido, Japan, and implications for evolution of the Pacific northwest. Isl. Arc 14, 582–598.
Ueda, Y., Aoki, K., 1968. K-Ar dating on the alkaline rocks from Nemuro, Hokkaido. J. J. Min. Petr. Econ. Geol. 59, 230–235 (in Japanese with English abstract).
Ulmer, P., 2001. Partial melting in the mantle wedge – the role of H_2O in the genesis of mantle-derived ‘arc-related’ magmas. Phys. Earth Planet. Inter. 127, 215–232.
van Hinsberg, V.J., Franz, G., Wood, B.J., 2017. Determining subduction-zone fluid composition using a tourmaline mineral probe. Geochem. Persp. Let. 3, 160–169. https://doi.org/10.7185/geochemlet.1719.
Winchester, J.A., Floyd, P.A., 1977. Geochemical discrimination of different magma series and their differentiation products using immobile elements. Chem. Geol. 20, 325–343.
Yagi, K., 1969. Petrology of the alkali dolerites of the Nemuro peninsula. Japan. Geol. Soc. Am. Mem. 115, 103–147.
Yatsuka, S., Okamura, S., Sakamoto, I., Azuma, T., Kim, Y., Ikeda, Y., 2010. Diverse geochemical signatures in MORB-like basalts dredged from the trench of the Ogasawara Ridge and the Hahajima Seamount –Implications for the origin of the tectonic event in the Izu-Bonin fore arc–. Jpn. Maga. Mineral. Petrol. Sci. 39, 171–189 (in Japanese with English abstract).
Yutani, T., Hirano, N., 2015. The Alkaline Magmas Intruded Into the Nemuro Group. The 122th Annual Meeting of the Geological Society of Japan 2015 (Abstract R1-O-9 in Japanese).
Yuatani, T., Hirano, N., 2016. Temporal and Spatial Distribution of Cretaceous Shoshonites in the Proto-Kuril Forearc Basin. The 123th Annual Meeting of the Geological Society of Japan 2016 (Abstract R2-P-1 in Japanese).
Zou, H., Zindler, A., 1996. Constraints on the degree of dynamic partial melting and source composition using concentration ratios in magmas. Geochim. Cosmochim. Acta 60, 711–717.